西 南 交 通 大 学 学 报

第 55 卷 第 1 期
2020 年 2 月

JOURNAL OF SOUTHWEST JIAOTONG UNIVERSITY

Vol. 55 No. 1
Feb. 2020

ISSN: 0258-2724 **DOI：10.35741/issn.0258-2724.55.1.46**

Research article

Mechanical Engineering

ASSESSING FRICTION EFFECT DUE TO THE VISCOSITY BETWEEN THE ROTOR AND A ROTATING MACHINE CASE

评估由于转子和旋转机壳之间的粘性而产生的摩擦效果

Zuhair H. Obiad, Haideer Taleb Shomran, Mohammed Salih Hassan
Al-Mussaib Technical Institute / Al-Furat Al-Awsat Technical University,51009Babylon,iraq
Byblion, Iraq, Inm.zoh@atu.edu.iq, Inm.had1@atu.edu.iq, hs.muhamad@atu.edu.iq

Abstract

In the first part of this paper, a new type of profiled rotor that rotates a working machine is presented. The machine is able to function either clean or with a suspension fluid. The aim of this work is to study the strength needed to overcome the viscous friction of two pairs of surfaces: between the case and the top of the piston and between the walls of the case and the rotor side surface. This paper includes a graphical presentation of the power consumption in both cases. The final part of this paper highlights the advantages of rotating machines with two profiled rotors. A reference list, which highlights the ongoing research into rotating machines with profiled rotors, concludes this paper.

Keywords: Viscous Friction, Profiled Rotor, Rotating Machine

摘要: 在本文的第一部分中，提出了一种新型的可旋转工作机的异型转子。机器可以清洁或使用悬浮液运行。这项工作的目的是研究克服两对表面的粘滞摩擦所需的强度：壳体与活塞顶部之间以及壳体壁与转子侧面之间。 本文包括两种情况下功耗的图形表示。本文的最后一部分重点介绍了具有两个异型转子的旋转电机的优势。本文总结了一份参考清单，重点介绍了正在进行中的异型转子旋转机的研究。

关键词： 粘滞摩擦，异型转子，旋转机

I. Introduction

Research into the field of thermal and hydraulic machines is currently focused on rotating machines. These machines have numerous advantages, such as the lack of distribution elements (camshafts, valves, etc.) and the absence of a crank drive mechanism, which increases the mechanical and internal efficiency of the machine [18].

Fluid potential pressure energy is increased through the almost complete transfer of power supplied from the engine shaft to the fluid. An explanation for this phenomenon is as follows:

Torque $\vec{M} = \vec{b} \cdot \vec{F}$ becomes $M = b \cdot F \sin \alpha$, where b is the arm of the force *(F)* and α is the angle between the force (*F*) and the arm of the force.

In this study, the arm of the force is the radius of the rotor + half of the rotating piston height and angle α = 90°, during the entire rotation. This study focuses on rotating volumetric operating machines that have a profiled rotor.

The constructive solutions included in this paper can be used as both a blower and a pump, thus explaining the term rotating machine.

The experimental work in this research was carried out in the laboratory of the Department of Thermotechnics, Engines, Thermal and Refrigeration Plants at the University (Politehnica) of Bucharest.

II. The Constructive Solution and Working Principles of the Machine

The machine's double-profiled rotors rotate in the opposite direction inside the case simultaneously (3, 8), as shown in Figure 1, which is driven by a pair of gearwheels. These two gearwheels form a cylindrical gear with straight teeth, and are mounted on external shafts (5) and (9). When there is rotational movement, the pistons (4) enter the adjoining rotor cavities. The profile form of the rotor is provided in [1], [2]. The manufacturing technology is provided in [3], [4]. The rotating pistons (4) act as a connector (1) for discharging (7). Using the values from this figure, the rate of flow and the power for driving are calculated as following [5], [6], [7]:

$$\dot{V} = \pi l z (2.r_r + z).\frac{n}{30}[\frac{m^3}{s}] \quad (1)$$

$$P_m = \dot{V}.\Delta p = \pi l z (2.r_r + z).\frac{n}{30}.\Delta p [W] \quad (2)$$

where n is the machine rotation, and $\Delta p$is the pressure increase between the suction and the discharge (N/m^2).

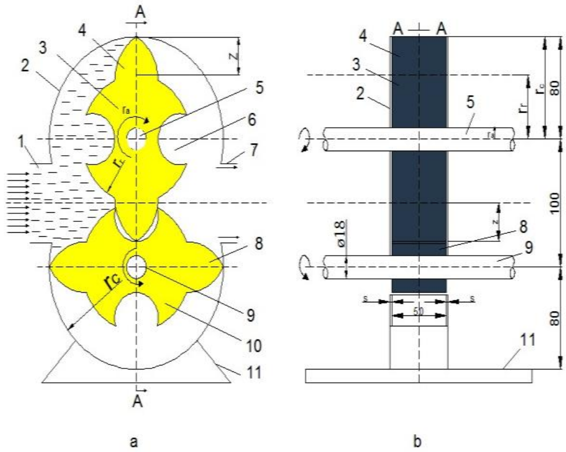

Figure 1. a - The blower cross section, b - The blower longitudinal section: 1. Gas section connection; 2. Upper case; 3. Upper rotor; 4. Rotating piston; 5. Driven shaft; 6. Cavity; 7. Gas discharge connection; 8. Lower rotor; 9. Driven shaft; 10. Surface of contact between rotor and the wall of case; 11. Support, r_a : Shaft radius, r_r : Rotor radius, z: Piston height

III. Calculation of the Power Consumed by the Viscous Friction between the Case and the Top of a Rotating Piston

The consumed power values are obtained for one rotor during one rotation, with one rotor piston revolving in a semi-cylindrical case. As shown in Figure 2a, the size of the gap between the case and the top of the piston is (x l), s = 0.01 x 〖10〗^(-3) m [8], and the rotor length is (l) = 50 x 〖10〗^(-3)m. A linear fluid velocity distribution is assumed for the fluid inside the gap, as shown in Figure 2b, and at point M the velocity of the fluid is

$$w = \omega.r_p \ [\frac{m}{s}] \quad (3)$$

where
ω is the angular velocity (rad/s) and
r_p is the radius of piston (m).

The viscous friction tangential to the effort results from relations [9], [10], [11], while the velocity of the fluid at point N is zero

$$\tau = \eta \frac{\partial w}{\partial z} = \eta \frac{w_M}{r_c - r_r} = \eta \frac{\omega r_p}{s} \quad (4)$$

where
r_c is the radius of case (m) and
η is the fluid dynamic viscosity (N.s/m^2).

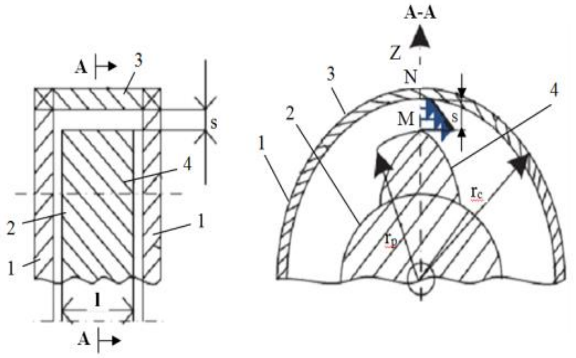

a b

Figure 2: The computing notations: 1. Walls of the case; 2. Rotor; 3. Rotating piston

Relation [12] gives the viscous friction between the case and the top of the piston

$$F_f = \tau . S \, [N] \tag{5}$$

where *S* is the friction surface in a radial direction. It is equal to the radius (r_p) and half of the length of the cylinder (*l*):

$$S = \pi . r_p . l \, [m^2] \tag{6}$$

When relations [4] and [6] are included into [5], the result is the following:

$$F_f = \eta \frac{\pi . \omega . r_p^2 . l}{s} . [N] \tag{7}$$

Relation [11] gives the friction torque between the fluid and the top of the piston:

$$M_f = F_f . r_p = \eta \frac{\pi . \omega . r_p^3 . l}{s} \, [N] \tag{8}$$

The calculation of mechanical power needed to overcome the viscous friction for a single rotor is [13]:

$$P_1 = \omega . M_f = \eta \frac{\pi . \omega^2 . r_p^3 . l}{s} \, [W] \tag{9}$$

The power needed to overcome the viscous friction on the radial surface is different since the machine has two rotors. The formula is as follows:

$$P_{m,r} = 2P_1 = \eta \frac{2 . \pi . \omega^2 . r_p^3 . l}{s} \, [W] \tag{10}$$

Equation (10) demonstrates that $P_{m,r}$ influences the value of η and ω^2 .

Water is used as the working fluid for a specific calculation [14]:

$$\eta = 10.04 . 10^{-4} \, [\frac{N.s}{m^2}]$$

Knowing that

$$r_p = r_c - s = (50 - 0.01).10^{-3} = 49.99.10^{-3} m$$

selecting $n_r = 100 \; rpm$

$$\omega = \frac{2.\pi.n_r}{60} = \frac{2.\pi.100}{60} = 10.47 \; rad/s \tag{11}$$

from relation [10], the power is obtained:

$$P_{m,r} = 10{,}04.10^{-4} \frac{2.3{,}14.(10.47)^2}{0.01.10^{-3}} \cdot \frac{(49{,}99.10^{-3})^3.50.10^{-3}}{0{,}01.10^{-3}} = 0.4317 (W)$$

Table 1 shows the results of the calculations for $n_r = 300{,}500{,}700{,}900 \; rpm.$

Table 1.
Values of $P_{m,r} = f(n_r)$

nr [rpm]	100	300	500	700	900
ω [rad/s]	10.47	31.416	52.359	73.303	94.247
***$P_{m,r}$* [w]**	0.431	3.888	10.791	21.151	34.964

Figure 3 shows a plotted curve $P_{m,r} = f(n_r)$ with the results from Table 1.

For a value $\eta = ct$, $P_{m,r}$ rises in a parabolic shape as the rot/min of the machine increases (Figure 3).

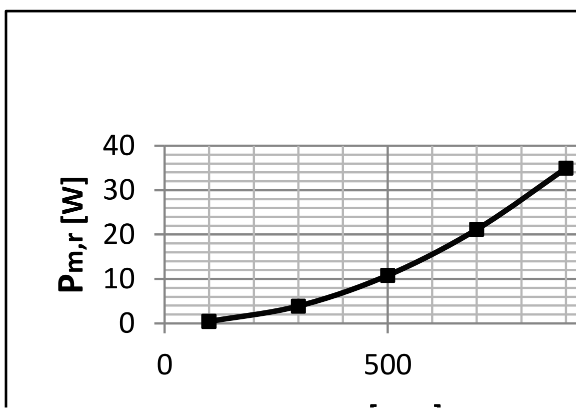

Figure 3. $P_{m,r} = f(n_r)$ for water

IV. Calculation of the Power Consumed by the Viscous Friction between the Case Side Walls and the Rotors

The calculation was based on the following hypotheses:

– The friction between the top of piston and the case can be disregarded.

– The areas used in this calculation are from r_a to r_r (Figure 4) as the rotor front surface fills the cavity inside the piston.

– The fluid velocity at each point on the rotor front surface is equal to the velocity of the rotor.

– The point's velocity on the surface of the disk is between

$$w_a = \omega . r_a \text{ and } w_r = \omega . r_r [m/s] \tag{12}$$

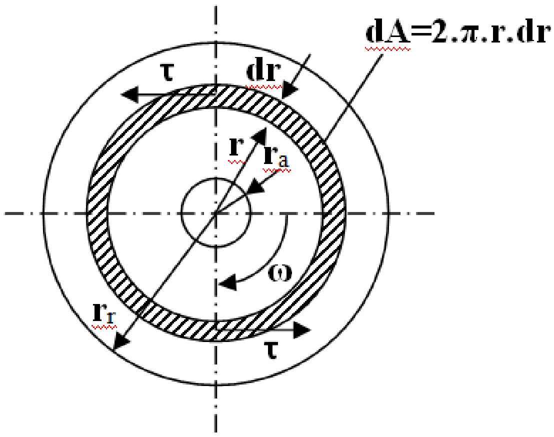

Figure 4. The plan view of a rotor portion

It is necessary to specify the power consumed by the viscous friction between the rotor's front surfaces and the walls of the case.

The primary known information is as follows:

– The rotor is mounted on a shaft with radius $r_a = 9.10^{-3}\, m$

– The exterior radius of the motor (r_r) is 50 x 10^{-3}m.

– The angular velocity is for a certain disk rot/min.

– The fluid dynamic viscosity at (t = 20°C) for water is

$$\eta = 10.04.10^{-4} \frac{N.s}{m^2};$$

– The gap value (s) between the walls of case and disk equals to 0.01 x 10^{-3} m according to the numerical controlled center precision processing [8].

The calculation is performed for a single rotor. The elementary resistant torque owing to the viscous friction between the case two walls and the rotor is as follows [12]:

$$dM_r = 2r.dF_f \tag{13}$$

In the aforementioned equation, F_r denotes the viscous friction force.

$$dF_f = \tau dA \tag{14}$$

In the equation above, τ signifies the tangential effort, while dA represents the elementary surface area, as depicted in Figure 2.

$$dA = 2\pi r.dr \tag{15}$$

Moreover, the Newton formula is used to calculate the shear stress (tangential tension) owing to the viscosity fluid [10]:

$$\tau = \eta \frac{dw}{dy} \tag{16}$$

Figure 5 demonstrates that the *y* coordinate is perpendicularly measured on the disk's surface.

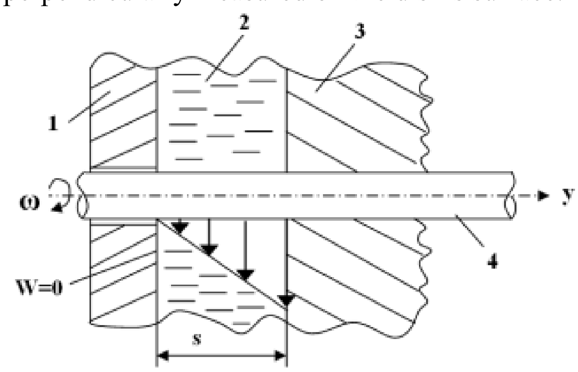

Figure 5. Computing section: 1. Case; 2. Fluid thin layer; 3. Disk of rotor; 4. Shaft

Further, the velocity gradient expression for the boundary layer with a thickness of (s) and a linear change is as follows:

$$\frac{dw}{dy} = \frac{\omega . r}{s} \tag{17}$$

Consequently, equation (16) becomes the can be represented as follows: $\tau = \eta \frac{\omega r}{s}$

(18)

Using equations (15) and (18), we can derive equation (14):

$$dF = \eta \frac{\omega . r}{s} .2\pi r dr = 2\pi r^2 \eta \frac{\omega}{s} dr \tag{19}$$

Through the use of theory of dynamic boundary layer [15], [16], a more exact calculation for dF_r is obtained.

From equations (13) and (19), the following can be determined:

$$dM_r = 2r.2\pi r^2 \eta \frac{\omega}{s} dr \tag{20}$$

$$\int_0^M dM_r = \int_{r_0}^{r_r} \frac{4.\pi.\omega.\eta.r^3}{s} dr \tag{21}$$

$$M_r = \frac{\pi.\eta.\omega}{s}(r_r^4 - r_a^4)\ [N.m] \tag{22}$$

The calculating relation of the consumed power for overcoming the viscous friction for a single rotor (from mechanics) is demonstrated below:

$$P_{1r} = M_r.\omega\ [W] \tag{23}$$

The consumed power via the viscous friction (P_m) for the entire machine is as follows:

$$P_{m,f} = 2.P_{1r}\ [W] \tag{24}$$

The result after introducing equations (22) and (23) into equation (24) is given below:

$$P_{m,f} = 2.\frac{\pi\eta\omega^2}{s}(r_r^4 - r_a^4)\ [W] \tag{25}$$

The value of (P_m) is influenced by (η) and (ω^2), as shown in equation (25), for a specific constructive solution.

In case the rotating machine is a pump that circulates water at an rpm of 100 rot/min, similar to that of equation (11), $\omega = 10.47\ rad/s$.

The result after replacement in equation (25) is as follows:

$$P_{m,f} = 2.\frac{3.14.10.04.10^{-4}.(10.47)^2}{0.01.10^{-3}}$$
$$\left[(50.10^{-3})^4 - (9.10^{-3})^4\right] = 0.431\ [W]$$

Table 2 presents the results pertaining to the calculation of $P_{m,f}$ for other values of n_r.

Table 2.
Values of $P_{m,r} = f(n_r)$

n_r [rpm]	100	300	500	700	900
ω [rad/s]	10.47	31.416	52.359	73.303	94.247
P_{mf} [w]	0.431	3.888	10.791	21.151	34.964

Based on the results shown in Table 2, the curve $P_{m,f} = f(n_r)$ is plotted in Figure 6.

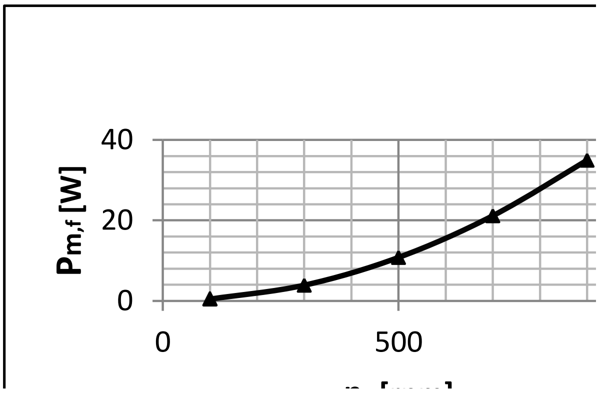

Figure 6. $P_{m,f} = f(n_r)$ for water

The graphs depicted in Figures 3 and 6 are overlapped in Figure 7.

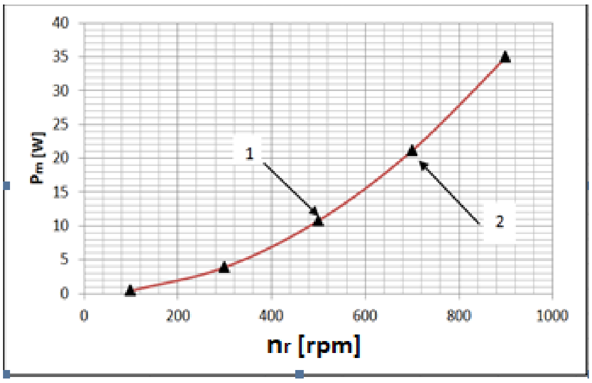

Figure 7. 1- $P_{m,r} = f(n_r); 2 - P_{m,f} = f(n_r)$

As observed in Figure 7, the consumed power for overcoming radial and frontal frictions is roughly equal.

The whole power needed for overcoming the viscous friction will be:

$$P_m = P_{m,r} + P_{m,f}\ [W] \tag{26}$$

Table 3 shows a sum of the data in Table 1 and Table 2.

Table 3.
Values of $P_{m,r} = f(n_r)$

n_r [rpm]	100	300	500	700	900
P_{mf} [w]	0.862	7.776	21.582	42.302	69.982

Based on the results in Table 3, the curve $P_m = f(n_r)$ is plotted in Figure 8. If the rpm of the machine increases, the consumed power for overcoming the viscous friction increases as well Figure 8. The influence of this consumed power is very small [17]. The consumed power increases when the machine rpm increases.

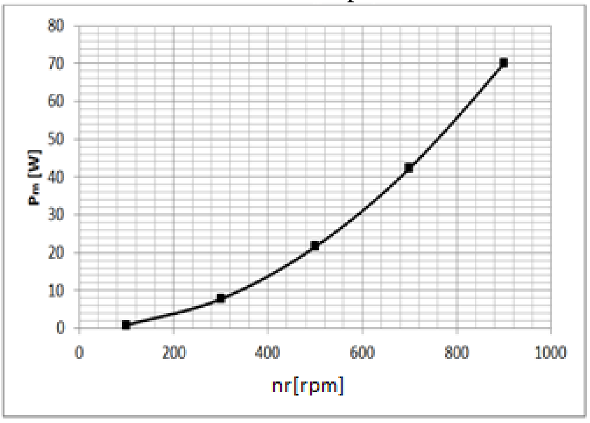

Figure 8. $P_m = f(n_r)$

V. Conclusions

1. η and ω2 influence the consumed power for overcoming the viscous friction, for a constructive solution.

2. Additives must be added to lower the dynamic viscosity of the fluid to reduce the consumed power. The value of ω is preferred to be as low as possible and is influenced by the operating system of the rotating machine.

3. The rotor architecture is determined via *rp* and *l*. By reducing r_r and increasing *l*, the *Pm* power decreases, as the friction upon the frontal surface and the viscous friction upon the radial surface are of the same order of magnitude.

4. The value of gap *s* between the case and the moving rotors has a great effect on the *Pm* value. CNC execution of the rotor can reduce this influence, as it is more rigorous.

5. Other utilizations and functions are explored for the new type of working machine presented in this study. Any fluid can be circulated by this machine.

6. The machine driving power depends on the nature of the fluid, which can be oil, water or air.

7. The present paper is a contribution to the experimental and theoretical research in the rotating machine field with an application to the study of profiled rotors.

References

[1] COSTACHE, A. and BĂRAN, N. (2008) Computation method for establishing the contour of a new type of profiled rotor. *University Politehnica of Bucharest Scientific Bulletin Series D: Mechanical Engineering*, 70 (3), pp. 93-102.

[2] BĂRAN, N., MOTORGA, A., and COSTACHE, A. (2008) Computing elements regarding the architecture of a profiled rotor. *Termotehnica*, 1, pp. 59-63.

[3] BĂRAN, N., BESNEA, D., SIMA, T., DETZORTZIS, A., and CARNARU, C. (2013) Manufacturing Technology for a New Type of Profiled Rotor. *Advanced Materials Research*, 655-657, pp. 235-240.

[4] BĂRAN, N., DONŢU, O., BESNEA, D., and COSTACHE, A. (2004) Constructive elements and technological procedures used in the construction of a new type of rotating compressor. *Romanian Review of Precision Mechanics, Optics & Mechatronics*, 25, pp. 265-268.

[5] DETZORTZIS, A., BĂRAN, N., and HAWAS, M. (2013) Influence of the profiled rotor design on the performance of rotating machines. *Termotehnica*, 2, pp. 127-132.

[6] BĂRAN, N., DESPINA, D., BESNEA, D., and DETZORTZIS, A. (2012) Theoretical and experimental researches regarding the performances of a new type of rotating machine with profiled rotors. *Advanced Materials Research*, 488-489, pp. 1757-1761.

[7] BĂRAN, N. (2000) Computing elements for a new type of rotating working machine with profiled pistons. *Romanian Review of Chemistry*, 51 (4), pp. 318-321.

[8] TCACENCO, V. (2005) Alzmetall vertical shaft processing centers. *Technical and Technology Journal*, 4, pp. 16-17.

[9] ANDERSON, E. (1993) *Thermodynamics*. Boston, Massachusetts: PWS Publishing Company.

[10] ACHESON, D.J. (1990) *Elementary Fluid Dynamics*. Oxford: Clarendon Press.

[11] ISBĂŞOIU, C.-T. (2011) *Treatise of Fluid Mechanics*. Bucharest: AGIR Publishing House.

[12] VOINEA, R., VOICULESCU, D., and

CEAUŞU, V. (1983) *Mechanics*. Bucharest: Didactic and Pedagogical Publishing House.

[13] BĂRAN, N., CĂLUŞARU, I., and DETZORTZIS, A. (2012) Research regarding the testing of a new type of rotating machine with profiled rotors. *Journal of Material Science and Engineering*, 2 (3), pp. 372-376.

[14] DOBROVICESCU, A., BĂRAN, N., and CHISACOF, A. (2009) *Technical Thermodynamics Fundamentals*. Bucharest: Politehnica Press Publishing House.

[15] SCHLICHTING, H. and GERSTEN, K. (2000) *Boundary-Layer Theory*. Berlin: Springer.

[16] CONSTANTINESCU, N. (1987) *Dynamic of Viscous Fluids in Laminar Flow Conditions*. Bucharest: Romanian Academy Publishing House.

[17] BĂRAN, N., DUMINICĂ, D., BESNEA, D., and DETZORTZIS, A. (2012) Theoretical and experimental researches regarding the performances of a new type of rotating machine with profiled rotors. *Advanced Materials Research*, 488-489, pp. 1757-1761.

[18] WANG, J., LI, J., WU, B., and ZHANG, Y. (2015) Calculation Method for Rotor Slot Leakage Inductance of Virtual-Slot Short-Pitch Wave Winding. *Journal of Southwest Jiaotong University*, 50 (3), pp. 405-409.

参考文:

[1] COSTACHE， A. 和 BĂRAN， N.（2008）建立新型异形转子轮廓的计算方法。布加勒斯特大学政治科学通报系列 D：机械工程，70（3），第 93-102 页。

[2] N. BĂRAN，A。MOTORGA 和 A. COSTACHE（2008）关于异型转子结构的计算元素。热工学，1，第 59-63 页。

[3] N. BĂRAN，BESNEA，D。SIMA，T。DETZORTZIS 和 C. CARNARU（2013）一种新型异形转子的制造技术。先进材料研究，655-657，第 235-240 页。

[4] N.BĂRAN，O.DONŢU，D。BESNEA 和 A. COSTACHE（2004）新型旋转压缩机的构造中使用的构造要素和技术程序。罗马尼亚精密机械，光学与机电一体化，25，第 265-268 页。

[5] DETZORTZIS，A.，BĂRAN，N. 和 HAWAS，M.（2013）异型转子设计对旋转机械性能的影响。热工学，2，第 127-132 页。

[6] B. RAN，北卡罗来纳州，DESPINA，D.，BESNEA，D。，和 DETZORTZIS，A。（2012）关于新型异形转子旋转机械性能的理论和实验研究。先进材料研究，488-489，第 1757-1761 页。

[7] BĂRAN，N.（2000）一种新型的异形活塞旋转工作机的计算元素。罗马尼亚化学评论，51 (4)，第 318-321 页。

[8] TCACENCO，V.（2005）阿尔兹金属立轴加工中心。技术和技术杂志，4，第 16-17 页。

[9] ANDERSON，E。（1993）热力学。马萨诸塞州波士顿：PWS 出版公司。

[10] ACHESON，D.J。（1990）基本流体动力学。牛津：克拉伦登出版社。

[11] ISBĂŞOIU，C.-T。（2011）流体力学论文。布加勒斯特：阿吉尔出版社。

[12] VOINEA，R.，VOICULESCU，D. 和 CEAUŞU，V.（1983）力学。布加勒斯特：教学法和教学出版社。

[13] N. BĂRAN，I。CĂLUŞARU 和 A. DETZORTZIS（2012）研究一种新型异形转子旋转机的测试。材料科学与工程学报，2（3），第 372-376 页。

[14] DOBROVICESCU，A.，BĂRAN，N. 和 CHISACOF，A.（2009）技术热力学基础。布加勒斯特：政治出版社。

[15] SCHLICHTING，H. 和 GERSTEN，K.（2000）边界层理论。柏林：施普林格。

[16] CONSTANTINESCU，N.（1987）层流条件下的粘性流体动力学。布加勒斯特：罗马尼亚科学院出版社。

[17] B. RAN，N.，DUMINIC，D.，BESNEA，D。和 DETZORTZIS，A。（2012）关于新型异形转子旋转机械性能的理论和实验研究。先进材料研究，488-489，第 1757-1761 页。

[18] 王健，李健，吴武，张 Y.（2015）虚拟槽短节距绕组转子槽漏感的计算方法。

西南交通大学学报，50（3），第 405-409 页。